Electronic Supplementary Material (ESI) for Dalton Transactions.
This journal is © The Royal Society of Chemistry 2016

Supplementary Information for manuscript:

Self-assembly synthesis, structure, topology, and magnetic properties of a mononuclear Fe(III)-violurate derivative: A combined experimental and theoretical study

Rupak Banik,‡[a] Subhadip Roy,‡[a] Ľubor Dlháň,[b] Ján Titiš,*[c] Roman Boča,*[c] Alexander M. Kirillov,*[d] Adam D. Martin,[e] Antonio Bauza,[f] Antonio Frontera,*[f] Antonio Rodríguez-Diéguez,[g] Juan M. Salas,[g] and Subrata Das*[h]

[a.] *Department of Chemistry, National Institute of Technology (NIT) Agartala, Pin 799046, Tripura, India*

[b.] *Institute of Inorganic Chemistry, FCHPT, Slovak University of Technology, 81237 Bratislava, Slovakia*

[c.] *Department of Chemistry, FPV, University of SS Cyril and Methodius, 91701 Trnava, Slovakia. E-mail address: jan.titis@ucm.sk; roman.boca@stuba.sk*

[d.] *Centro de Química Estrutural, Complexo I, Instituto Superior Técnico, Universidade de Lisboa, Av. Rovisco Pais, 1049-001 Lisbon, Portugal. E-mail address: kirillov@tecnico.ulisboa.pt*

[e.] *School of Chemistry and the ARC Centre for Convergent Bio-Nano Science and Technology, The University of New South Wales, Sydney, Australia*

[f.] *Departament de Quimica, Universitat de les Illes Balears, Crta. de Valldemossa km 7.5, 07122 Palma de Mallorca (Baleares), Spain. E-mail address: toni.frontera@uib.es*

[g.] *Departamento de Quimica Inorganica, Facultad de Ciencias, Universidad de Granada, 18071 Granada, Spain*

[h.] *Department of Chemistry, National Institute of Technology (NIT) Patna, Ashok Rajpath, Patna-800005, Bihar, India. E-mail address: subrataorgchem@gmail.com; Tel.: +917677417481*

Table of contents:

1. Materials and methods

Synthetic reactions were performed in air. Violuric acid monohydrate was prepared using the synthetic method available in the literature.[1] All the other reagents were obtained from commercial sources and used without further purification. Elemental analyses (C, H and N) were performed using a Perkin-Elmer 2400 series II CHN analyzer. FT-IR spectrum was recorded on a Perkin-Elmer Spectrum 100 FT–IR spectrometer in KBr pellets. The DC magnetic data for **1** was taken by using the SQUID magnetometer (MPMS-XL7, Quantum Design) in the RSO mode of the detection. The susceptibility data was acquired at the applied field B_{DC} = 0.1 T and the raw data was transformed to the effective magnetic moment. The magnetization was taken at T = 2.0 and 4.6 K, respectively, and presented in the form of the magnetization per formula unit $M_1 = M_{mol}/N_A\mu_B$. The zero-field cooling magnetization and field cooling magnetization experiments (ZFCM/FCM) were conducted at the applied field of B = 10 mT between 2 - 100 – 2 K. The hysteresis loop was cycled at T = 2.0 and 5.0 K, respectively.

2. Discussion of Hirshfeld surface analysis

Hirshfeld surface analysis was undertaken using *Crystal Explorer 3.1*.[2] The structure contains three violuric acid molecules coordinated to an Fe(III) centre in an octahedral manner. Four water molecules and one pyridine are also present in the crystal structure. The fingerprint plot shows two large spikes, pointing towards the bottom left of the plot (Fig. S2). These spikes represent O···H interactions, which make up 59.7% of the Hirshfeld surface

(Fig. S3). This suggests that the structure is dominated by hydrogen bonds, as has been stated before in structure description. This is supported by the lack of any spikes along the $d_i = d_e$ diagonal, indicating no short H···H contacts (the proportion of H···H interactions is quite low, at only 8.1%, Fig. S4). Furthermore, no "wings" are observed on the fingerprint plot, which are often characteristic of C-H···π interactions. These C···H interactions only make up 6.8% of the Hirshfeld surface, Fig. S5. Interestingly, although C···C interactions only comprise 3% of the surface, two distinct populations of these contacts are present on the Hirshfeld surface, with the closer contacts (further towards the bottom left) due to interactions between the ligand and neighbouring pyridine molecules (as mentioned in the manuscript), Fig. S6.

The three violuric acid ligands are distinct, in their coordination distances and their interactions. For the first violuric acid, defined by N31 and O31 as defined in the manuscript, there are a number of short, O···H based contacts. N32-H32 has a close contact with an adjacent O23 (highlighted in orange, Fig. S7a). The other N-H on the pyrimidine ring, N33-H33, displays a close contact with a water molecule, O2W (Fig. S7b, highlighted in orange). Both carbonyls have close contacts with neighbouring hydrogens – O32 closely contacts a hydrogen from O1W (highlighted in orange in Fig. S7a) and O33 displays a bifurcate interaction (highlighted in orange in Fig. S7b), with both N12-H12 and N23-H23, from different neighbouring molecules.

The second violuric acid ligand, defined by N21 and O21, also displays predominantly hydrogen bonding short interactions, however this ligand also interacts with the pyridine solvent. N22-H22 has a close contact with O3W (Fig. S7a, highlighted in green). As mentioned previously, N23-H23 interacts with a neighbouring O33. The O22 atom has a short contact with an adjacent N13-H13 (both highlighted in purple, Fig. S7b). O23 has a bifurcate interaction (like the analogous oxygen in the first ligand), except in this case it is with N32-H32 and also H5SA from the pyridine. This hydrogen from the pyridine also interacts with O24, which suggests it has an important role in stabilising the conformation of this violuric acid ligand.

The final violuric acid ligand is defined by the atoms N11 and O11 coordinated to the iron centre. N11-O14 displays a short contact with one of the protons from O1W. The other proton from O1W has a short contact with the next carbonyl on the ligand, O13. This carbonyl also has an interaction with a proton from O2W (circled in purple, Fig. S7a). Interestingly, all of the oxygen molecules at this position (O13, O23 and O33) show bifurcate interactions, suggesting that this is a key area for stabilising the geometry and arrangement of the structure. N13-H13 interacts with O22, as described previously (highlighted in purple,

Fig. S7a). O12 interacts with protons form two water molecules, O3W and O4W (highlighted in green, Fig. S7b). It should now be noted that this ligand has a much higher proportion of interactions with solvent molecules (in this case, water) than either of the other ligands. N12-H12 has a close contact with O33, described previously. The pyridine solvent molecule, aside from the close contacts which have previously been described, has close contact with a proton from O4W.

3. Figures

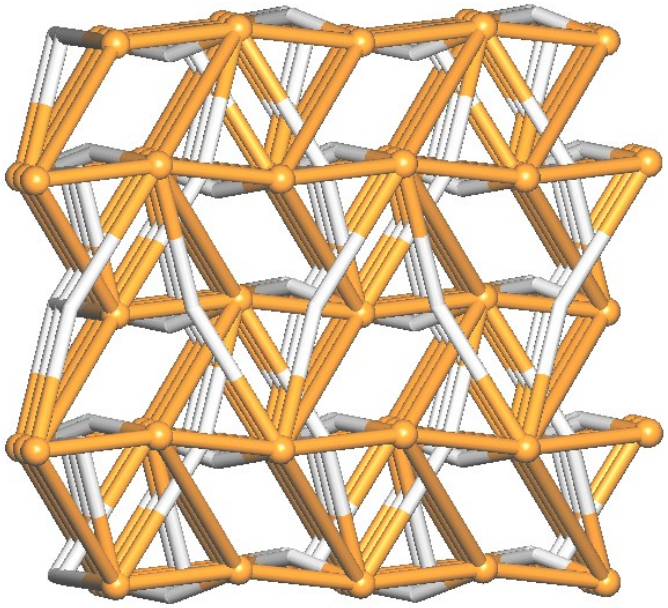

Fig. S1 Topological representation of the 3D H-bonded network driven by strong H-bonds between [Fe(H_2Vi)$_3$] units and crystallization H_2O molecules and showing a binodal 3,11-connected net with a unique topology defined by the point symbol of ($3^6.4^{23}.5^{16}.6^9.7$)($4^2.5$); rotated view along the *a* axis; color codes: centroids of 11-connected [Fe(H_2Vi)$_3$] molecular nodes (orange balls), centroids of 3-connected $(H_2O)_2$ nodes and 2-connected H_2O linkers (gray).

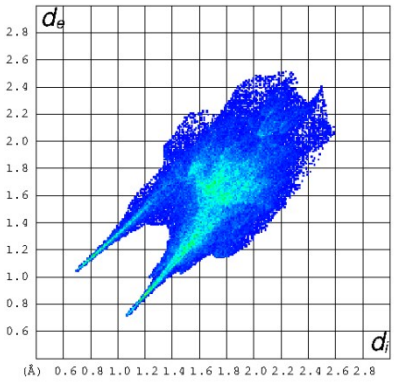

Fig. S2 Full fingerprint plot for $[Fe(H_2Vi)_3]$, displaying contacts from all interactions.

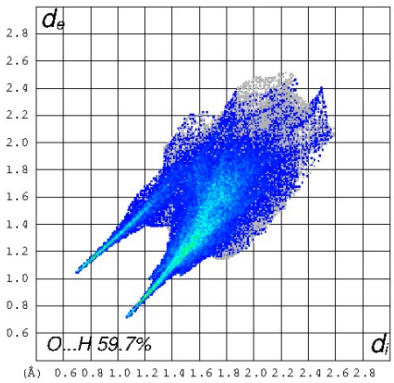

Fig. S3 Fingerprint plot highlighting O···H interactions present within $[Fe(H_2Vi)_3]$.

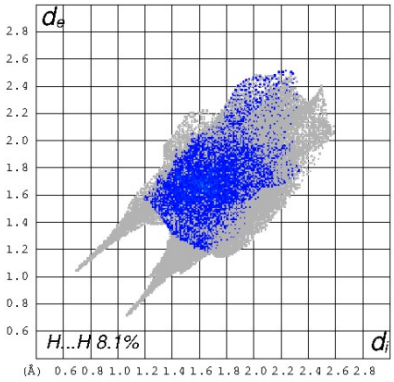

Fig. S4 Fingerprint plot highlighting H···H interactions present within $[Fe(H_2Vi)_3]$.

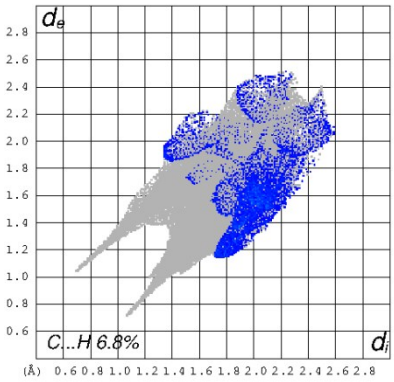

Fig. S5 Fingerprint plot highlighting C···H interactions present within $[Fe(H_2Vi)_3]$.

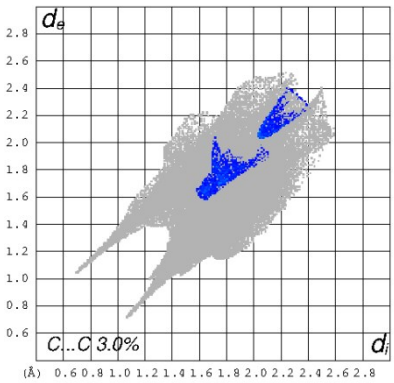

Fig. S6 Fingerprint plot highlighting C···C interactions present within $[Fe(H_2Vi)_3]$.

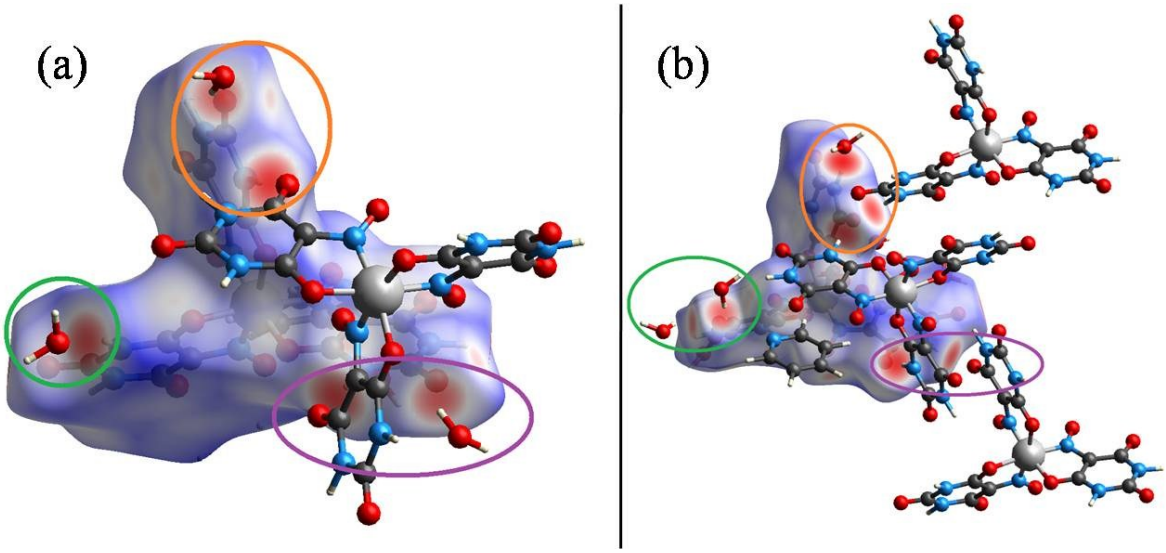

Fig. S7 (a,b) d_{norm} surface of $[Fe(H_2Vi)_3]$, showing close contacts for each of the coordinated violuric acid molecules, which interact with both neighbouring ligands and adjacent water molecules.

4. Tables

Table S1. Bond lengths for **1**.

Atom	Atom	Length/Å	Atom	Atom	Length/Å
Fe1	O11	1.9858(13)	N22	C21	1.352(2)
Fe1	O21	1.9813(14)	N22	C22	1.373(3)
Fe1	O31	1.9991(15)	N23	C22	1.362(3)
Fe1	N11	1.8668(16)	N23	C23	1.380(2)
Fe1	N21	1.8702(16)	N31	C34	1.369(3)
Fe1	N31	1.8823(16)	N32	C31	1.360(3)
O11	C11	1.253(2)	N32	C32	1.375(3)
O12	C12	1.216(2)	N33	C32	1.375(3)
O13	C13	1.223(2)	N33	C33	1.380(3)
O14	N11	1.250(2)	C11	C14	1.415(2)
O21	C21	1.255(2)	C13	C14	1.435(2)
O22	C22	1.213(2)	C21	C24	1.420(2)
O23	C23	1.229(2)	C23	C24	1.437(2)
O24	N21	1.248(2)	C31	C34	1.420(2)
O31	C31	1.253(2)	C33	C34	1.429(3)
O32	C32	1.214(3)	C3S	C4S	1.382(6)
O33	C33	1.236(2)	C3S	C2S	1.366(6)
O34	N31	1.249(2)	C4S	C5S	1.297(6)
N11	C14	1.360(2)	C5S	C6S	1.328(5)
N12	C11	1.356(2)	C5S	N6S	1.328(5)
N12	C12	1.370(2)	C6S	N1S	1.351(5)
N13	C12	1.363(3)	N1S	C2S	1.331(5)
N13	C13	1.383(3)	C2S	C1S	1.331(5)
N21	C24	1.369(2)	C1S	N6S	1.351(5)

Table S2. Bond angles for **1**.

Atom	Atom	Atom	Angle/°	Atom	Atom	Atom	Angle/°
O11	Fe1	O31	85.76(6)	O13	C13	C14	126.58(19)
O21	Fe1	O11	90.60(6)	N13	C13	C14	113.39(16)
O21	Fe1	O31	89.81(6)	N11	C14	C11	111.92(15)
N11	Fe1	O11	83.93(6)	N11	C14	C13	126.94(16)
N11	Fe1	O21	173.47(7)	C11	C14	C13	121.07(16)
N11	Fe1	O31	93.33(7)	O21	C21	N22	120.94(17)
N11	Fe1	N21	93.87(7)	O21	C21	C24	120.56(16)
N11	Fe1	N31	94.92(7)	N22	C21	C24	118.49(16)
N21	Fe1	O11	100.59(6)	O22	C22	N22	121.4(2)
N21	Fe1	O21	83.61(6)	O22	C22	N23	122.0(2)
N21	Fe1	O31	170.86(6)	N23	C22	N22	116.61(16)
N21	Fe1	N31	90.46(7)	O23	C23	N23	120.10(17)

N31	Fe1	O11	168.94(7)	O23	C23	C24	126.28(17)
N31	Fe1	O21	91.13(7)	N23	C23	C24	113.57(16)
N31	Fe1	O31	83.32(6)	N21	C24	C21	111.56(15)
C11	O11	Fe1	108.70(11)	N21	C24	C23	126.83(16)
C21	O21	Fe1	108.63(11)	C21	C24	C23	120.85(15)
C31	O31	Fe1	109.58(12)	O31	C31	N32	121.01(16)
O14	N11	Fe1	125.98(13)	O31	C31	C34	120.92(19)
O14	N11	C14	120.35(16)	N32	C31	C34	118.07(18)
C14	N11	Fe1	113.65(12)	O32	C32	N32	122.19(19)
C11	N12	C12	123.31(16)	O32	C32	N33	121.9(2)
C12	N13	C13	127.21(16)	N33	C32	N32	115.86(19)
O24	N21	Fe1	126.87(12)	O33	C33	N33	119.02(19)
O24	N21	C24	120.22(16)	O33	C33	C34	126.1(2)
C24	N21	Fe1	112.63(12)	N33	C33	C34	114.91(16)
C21	N22	C22	122.91(16)	N31	C34	C31	111.86(17)
C22	N23	C23	126.94(17)	N31	C34	C33	127.26(16)
O34	N31	Fe1	126.31(14)	C31	C34	C33	120.84(18)
O34	N31	C34	119.87(17)	C2S	C3S	C4S	119.4(3)
C34	N31	Fe1	113.82(12)	C5S	C4S	C3S	120.1(3)
C31	N32	C32	124.02(16)	C4S	C5S	C6S	120.7(4)
C32	N33	C33	126.20(18)	C4S	C5S	N6S	120.7(4)
O11	C11	N12	120.38(15)	C5S	C6S	N1S	120.9(3)
O11	C11	C14	121.02(15)	C2S	N1S	C6S	120.2(3)
N12	C11	C14	118.58(15)	N1S	C2S	C3S	118.8(4)
O12	C12	N12	122.07(19)	C1S	C2S	C3S	118.8(4)
O12	C12	N13	121.95(18)	C2S	C1S	N6S	120.2(3)
N13	C12	N12	115.97(17)	C5S	N6S	C1S	120.9(3)
O13	C13	N13	120.01(17)				

5. References

[1] N. A. Illán-Cabeza, A. R. García-García and M. N. Moreno-Carretero, *Inorg. Chim. Acta*., 2011, **366**, 262-267.

[2] S. K. Wolff, D. J. Grimwood, J. J. McKinnon, M. J. Turner, D. Jayatilaka and M. A. Spackman, CrystalExplorer (Version 3.1), University of Western Australia, 2012.